Formulation of Parameter–based Shape Sensitivities from Free–field Size Sensitivities

Afshin MIKAILI
James BERNARD

Department of Mechanical Engineering
Iowa State University
Ames, IA 50011, U.S.A.

ABSTRACT

Conventional finite–element–based structural shape optimization requires the calculation of grid sensitivities which are much more expensive to compute than size sensitivities. This paper presents an alternate method of shape optimization which is based on using size sensitivities (computed using MSC/NASTRAN, Version 66A) to guide shape redesign. In this method, a thin layer of plate elements is cast on selected free surfaces of structures modeled with solid elements, or in the case of structures modeled with plate elements, selected free edges are covered with a thin lining of beam elements. While the performance of the structure remains virtually unaffected by introducing these nearly zero section elements, the sensitivities of the structural response with respect to the thickness of these elements provide qualitative insight on the behavior of the structure as well as a quantitative basis for shape optimization. This paper also addresses the challenge of calculating parameter–based shape sensitivities (e.g., sensitivity with respect to a shaft diameter, or a shaft fillet radius) from the computed free–field size sensitivities. The method is applied to a pin geometry under two different static loading conditions.

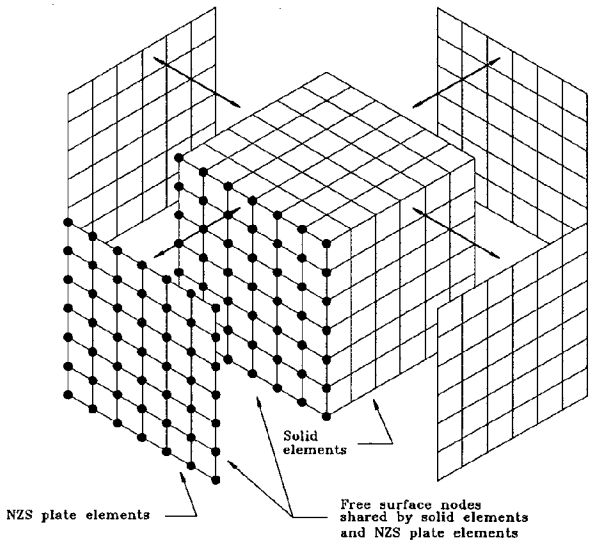

Figure 1: NZS shell elements coating the free faces of solid elements

Introduction

Conventional finite–element–based structural shape optimization requires the calculation of grid sensitivities. These sensitivities give quantitative measures on how the structural response varies as the coordinates of a grid point or a grouping of grid points are varied. Haftka and Grandhi [1] give a survey of the methods currently used for calculating grid sensitivities. Briefly, grid sensitivities are calculated either by differentiation of the finite element model, or by differentiation of the continuum equations. The former method has proven to be computationally expensive, while the latter method leads to numerical difficulties due to the need for the calculation of boundary integrals. The use of domain integrals instead of boundary integrals to alleviate the numerical difficulties results in calculations which are nearly as expensive as the former method.

An alternate method for shape optimization was proposed by Mikaili and Bernard [2]. In this method, a thin layer of plate elements is cast on selected free surfaces of structures modeled with solid elements, or in the case of structures modeled with plate elements, selected free edges are covered with a thin lining of beam elements. This is shown schematically by Figures 1 and 2. Finite element pre–processors (see, for example, Ref. [3]) typically provide efficient means of creating these elements on the free surfaces of user–selected elements. While the analysis results remain virtually unaffected by introducing these nearly zero section (NZS) elements, the sensitivities of the structural response with respect to the thickness of these elements provide qualitative insight on the behavior of the structure as well as a quantitative basis for shape optimization. Furthermore, these sensitivities are size sensitivities which are computed at a much lower computational cost than grid sensitivities.

Mikaili and Bernard [2] applied the NZS method to a cantilever beam under a transverse

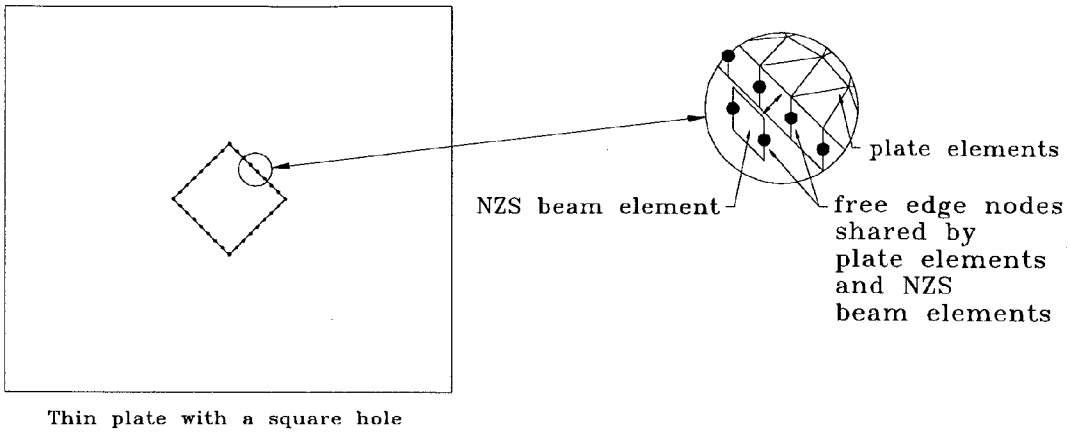

Figure 2: NZS beam elements lining the free edges of plate elements

gravitational load. Figures 3 and 4 show the 20" long, steel beam (modeled with hexagonal solid elements) with an initial uniform 3" X 3" cross–section, and the 0.05" thick plate elements coating the four sides of the beam. Figure 5 presents the contour plot of the sensitivity of the free end deflection with respect to the thickness of each NZS plate element. The new beam shape of Figure 6 was derived from these sensitivities and a grid movement formulation based on closed form, algebraic relations. Subsequent remeshing and finite element analysis of the new beam indicated a 63% reduction in the free end deflection.

In this application it was assumed that there were no imposed geometric constraints. In this "free–field" approach, the sensitivities were used directly to modify the location of the surface nodes with no geometric constraints on the movement of the nodes. However, oftentimes, due to manufacturing, aesthetic, or other considerations, structural shape optimization is limited to keeping the general shape characteristics of the structure unchanged. These constraints lead to the fact that only changes in the values of the dimensional parameters of the structure (e.g., a shaft diameter, or a fillet radius) are allowed. Therefore, there is a need to translate the free–field NZS sensitivity information to parameter–based sensitivities. This paper introduces a methodology for the formulation of parameter–based shape sensitivities from free–field size sensitivities.

Formulation of parameter–based shape sensitivities from free–field size sensitivities

Figure 7 shows a two dimensional cross section of a stepped shaft and the relocation of the surface nodes as the diameter of one section is changed from d_1 to d_2. Note that the mesh density is the same for the initial and modified designs. For example, there is an equal number of elements resolving the fillet region for both designs.

This criterion on the mesh makes it important to have access to an automated, parameter–based finite element pre–processor. There are many such programs available commercially.

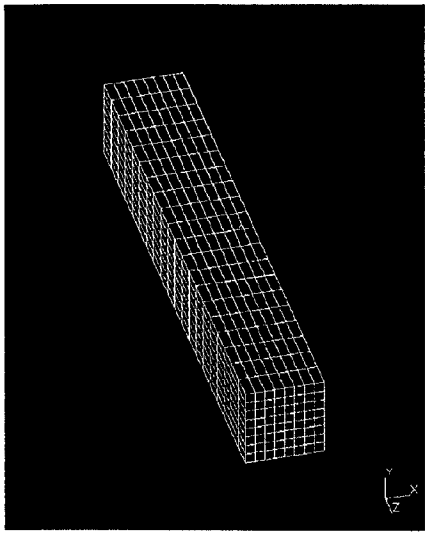

Figure 3: Finite element model of a 3" X 3" X 20" cantilever beam

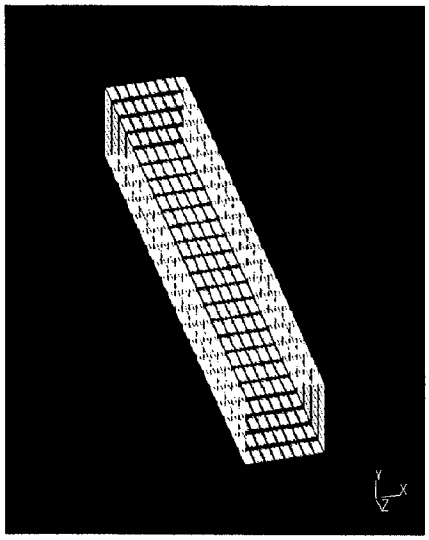

Figure 4: 0.05" thick NZS elements coating the sides of the beam (elements shrunk for display purposes)

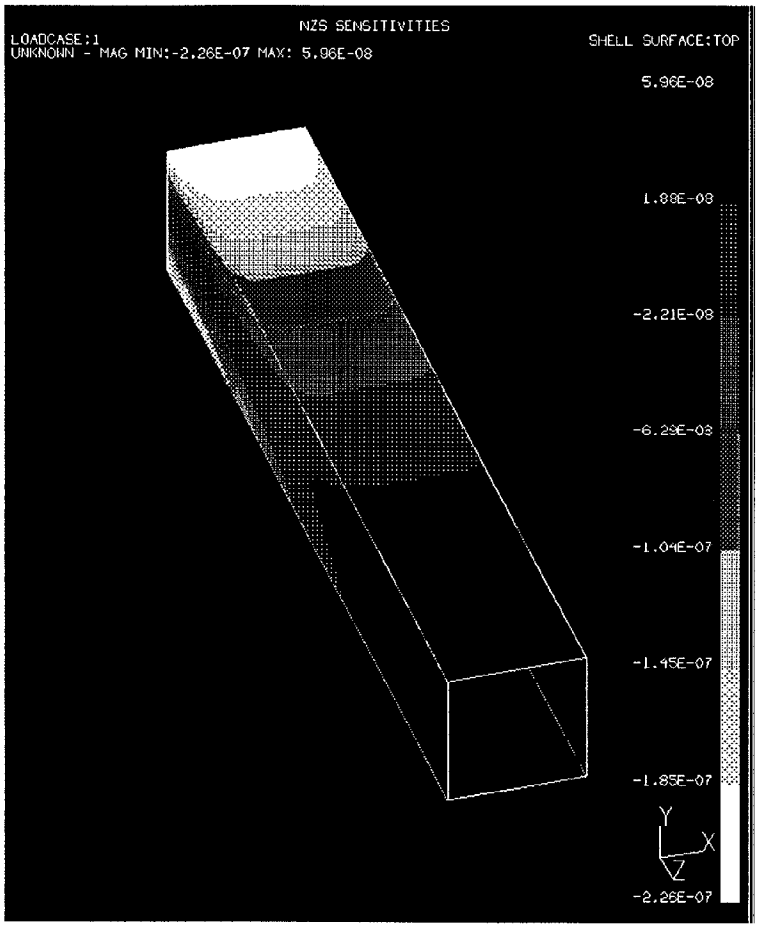

Figure 5: NZS sensitivities for the initial beam

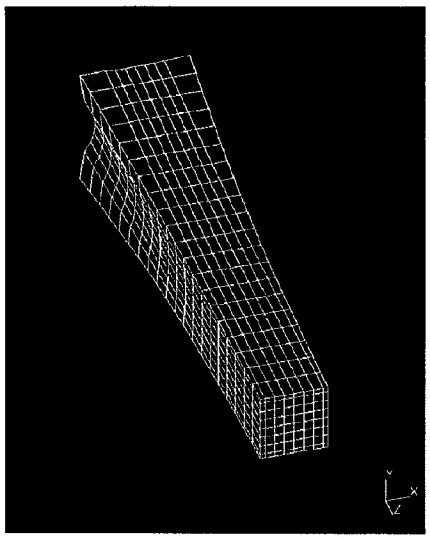

Figure 6: Modified cantilever beam

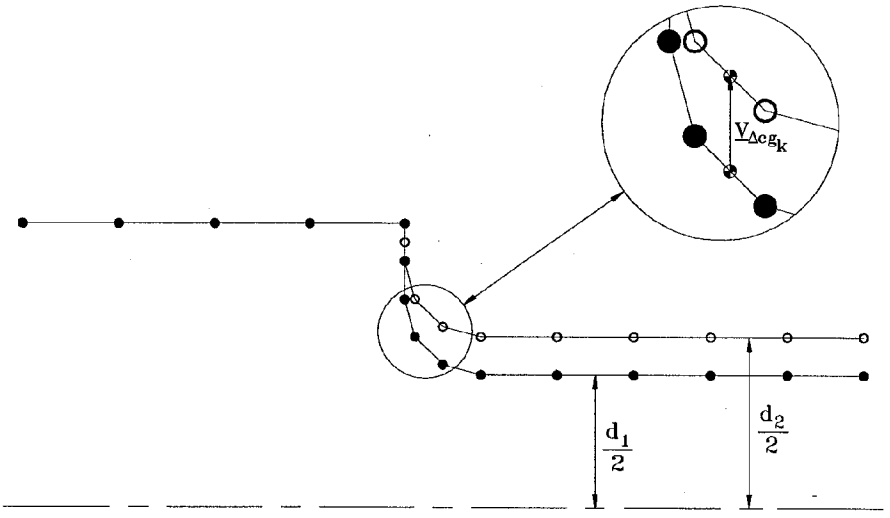

Figure 7: Relocation of shaft surface nodes with a change in shaft diameter (2D profile)

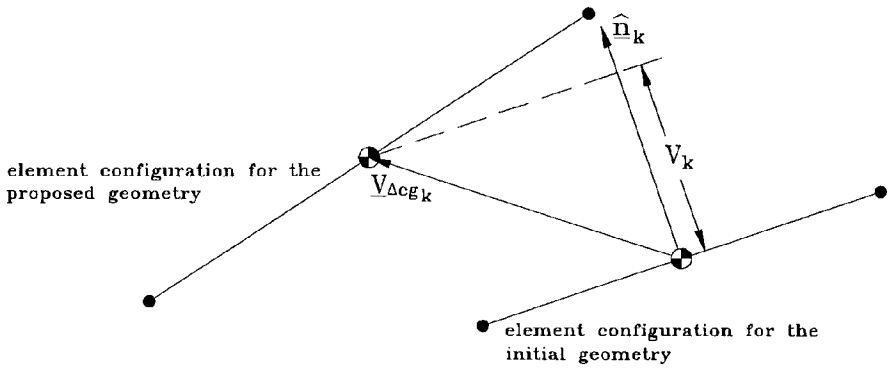

Figure 8: Effective material addition (2D)

(See, for example, Ref. [3].)

It should also be noted that the mesh for the modified design is not necessarily used for finite element analysis. This mesh is only used in calculating the displacement of the centroid of each finite element as a result of a change in one or more dimensional parameter.

As Figure 7 shows, the centroid of each (kth) NZS element undergoes a displacement of $\underline{V}_{\Delta cg_k}$. An effective thickness, V_k, can be calculated by projecting $\underline{V}_{\Delta cg_k}$ on the unit vector normal to the element in its initial configuration:

$$V_k = \underline{V}_{\Delta cg_k} \cdot \hat{\underline{n}}_k \tag{1}$$

Figure 8 gives a graphical representation of this equation. With the normal vector defined to point outward, a positive value from Equation 1 corresponds to addition of material while a negative value suggests removal of material.

The effective thicknesses, V_k, can then be used in a first order Taylor series expansion to calculate a predicted response for the lth response variable, R_{l_p}:

$$R_{l_p} = R_{l_o} + \sum_{k=1}^{N_k} \frac{\partial R_l}{\partial v_k} V_k \tag{2}$$

where R_{l_o} is the original response, and $\frac{\partial R_l}{\partial v_k}$ is the sensitivity of the lth response variable with respect to the kth NZS thickness.

Parameter–based sensitivities can, in turn, be calculated using:

$$\frac{\partial R_l}{\partial p_i} = \frac{R_{l_p} - R_{l_o}}{p_{i_p} - p_{i_o}} \tag{3}$$

where p_i represents a dimensional parameter (e.g., a shaft diameter) with p_{i_p} and p_{i_o} corresponding to the proposed and the original geometries, respectively. Once parameter–based sensitivities are calculated, first order structural optimization techniques (see, for example, Ref. [4, 5]) can be used for optimization.

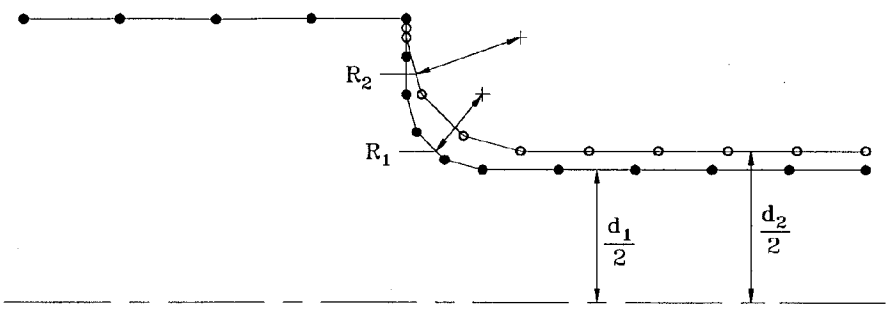

Figure 9: Relocation of shaft surface nodes with changes in shaft diameter and fillet radius (2D profile)

It is important to note that Equation 2 can be used with several simultaneous changes in dimensional parameters. For example, Figure 9 shows a case where both the fillet radius and the shaft diameter are changed. Equations 1, and 2 can still be used to predict the response of the structure. The p_i parameter of Equation 3 may then be some independent variable which determines both the shaft diameter and the fillet radius.

Case study: pin under point loading

The pin geometry of Figure 10 will be used as a case study. The geometry and the loading are symmetric across the midplane of the pin; therefore, as shown by Figure 11, a half–pin finite element model is used in the analysis. Symmetric boundary conditions are applied to the midplane nodes. The surface nodes lying along the threaded portion are constrained in all degrees of freedom. This figure also shows NZS plate elements coating the free faces of the solid elements. The interior nodes are only coupled by solid elements; therefore, they have no rotational degrees of freedom. However, the surface nodes are shared by plate elements as well as solid elements. These nodes have rotational degrees of freedom in addition to their translational degrees of freedom.

The first loading condition considered for the pin is a point load applied in the transverse direction at the top of the stem. Figures 12, 13, and 14 show contour plots of the maximum principal stress and the sensitivity of the stress in the solid element with the highest tensile stress, σ_h, with respect to the thickness of the plate elements of Figure 11.

A first order prediction model for σ_h is constructed using Equation 2:

$$\sigma_{h_p} = \sigma_{h_o} + \sum_{k=1}^{N_k} \frac{\partial \sigma_h}{\partial v_k} V_k \tag{4}$$

with V_k representing the effective thickness for the kth NZS plate element computed using Equation 1.

Figure 15 shows the relocation of the surface nodes of the pin as the stem radius is reduced to 3.75 mm from its nominal value of 4.875 mm. For this change in the pin geometry,

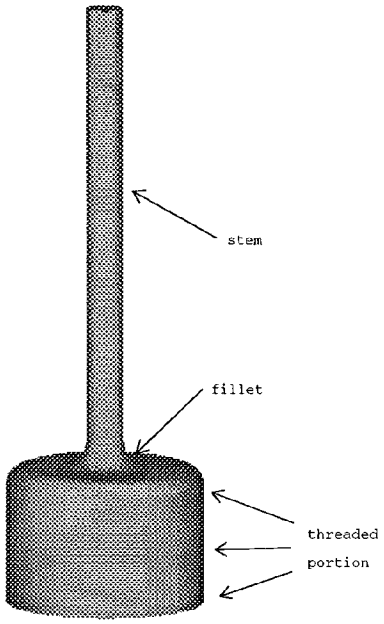

Figure 10: Pin geometry

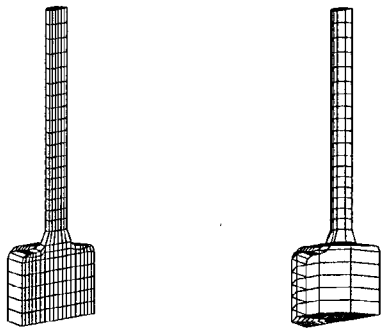

Figure 11: Pin finite element model and NZS plate elements

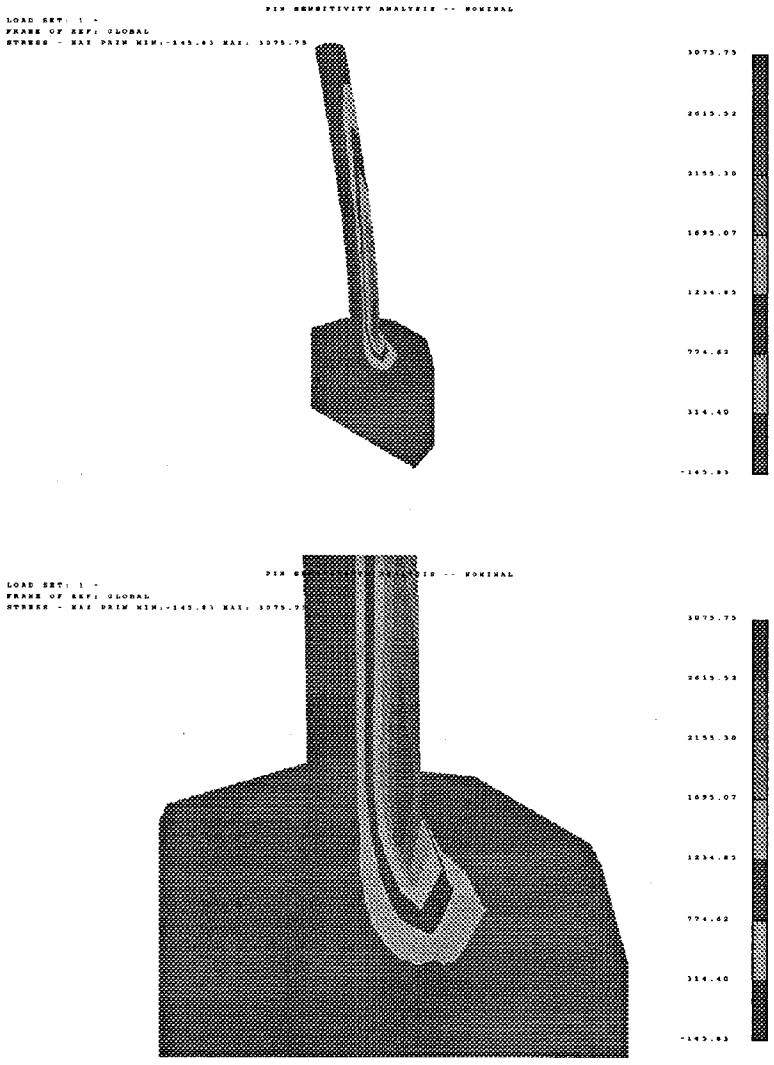

Figure 12: Maximum principal stress distribution (point loading)

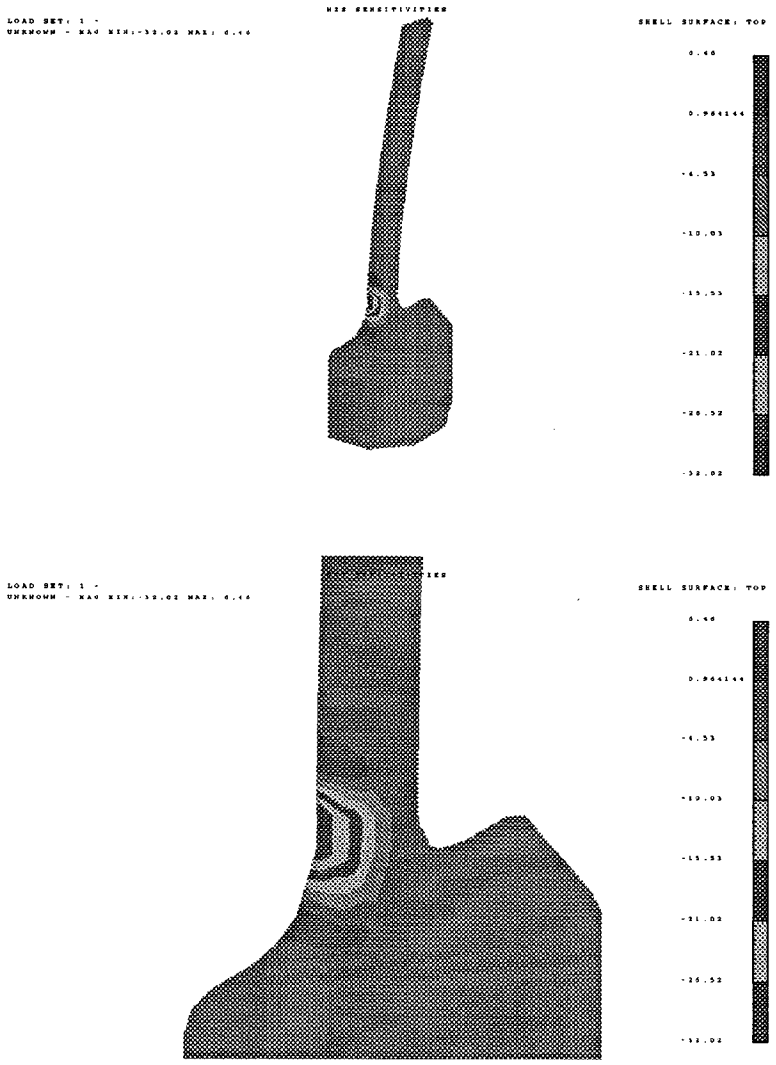

Figure 13: Sensitivity distribution, tension side (point loading)

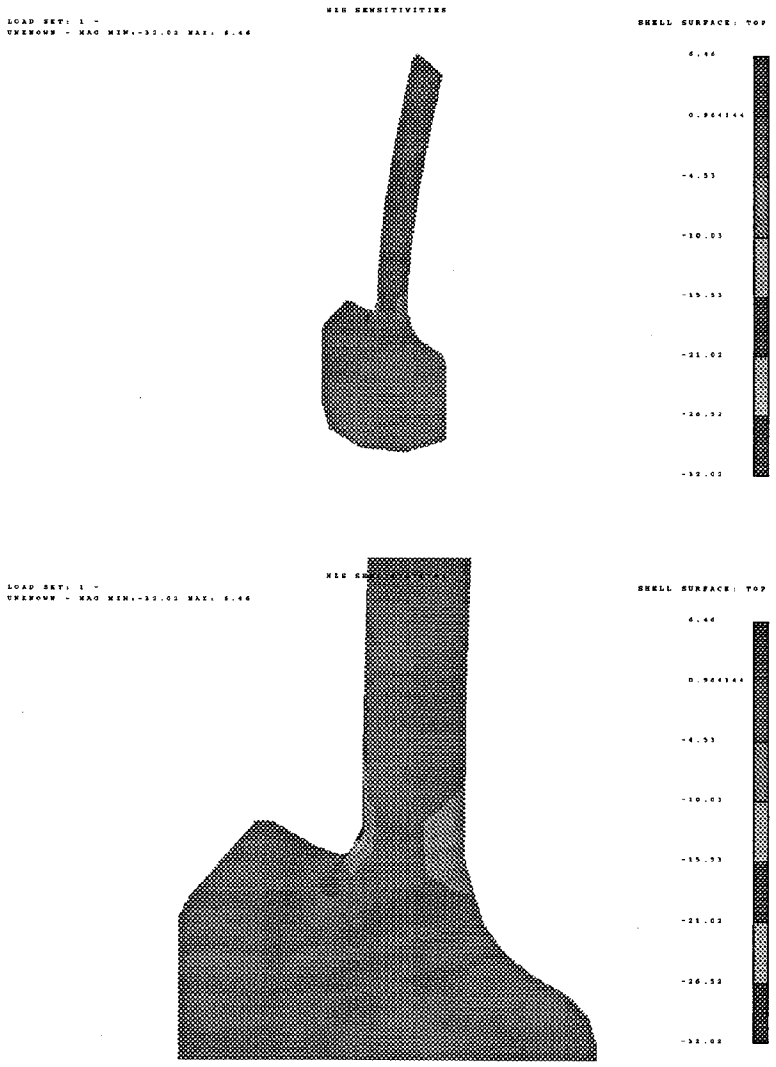

Figure 14: Sensitivity distribution, compression side (point loading)

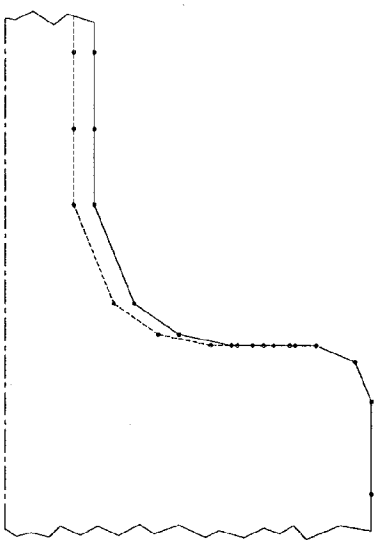

Figure 15: Relocation of the pin surface nodes (2D profile)

Table 1: Stress results for the pin geometry under point loading

Design number	Stem radius (mm)	Fillet radius (mm)	FEA σ_h (kPa)	Predicted σ_h (kPa)	Deviation (kPa)
1 (nominal)	4.875	7.5	2372.7	—	—
2	3.75	7.5	5137.1	4574.3	562.8
3	3.75	5.0	5282.8	4511.7	771.1
4	6.0	5.0	1323.0	108.6	1214.4

V_k assumes a negative value for the elements along the stem and the fillet and a value of zero elsewhere. This new design is designated as Design 2 in Table 1.

Table 1 shows that for Design 2, there is a 562.8 kPa deviation between the σ_h predicted using Equation 4, and the corresponding value calculated by a FEA re–analysis. This table also presents calculations for two additional pin designs. In Design 3 the fillet radius is changed to 5.0 mm from its nominal value of 7.5 mm while the stem radius is set equal to that of Design 2. The deviation between predicted and calculated stress is 771.1 kPa which is slightly higher than that of Design 2. In Design 4, where the stem radius is increased to 6.0 mm, the deviation is 1214.4 kPa.

To investigate reasons for these deviations, several more FEA runs were conducted with the fillet radius kept constant at the nominal value of 7.5 mm and the stem radius varying from 3 mm to 7 mm. Figure 16 presents results. As expected, the accuracy of the linear

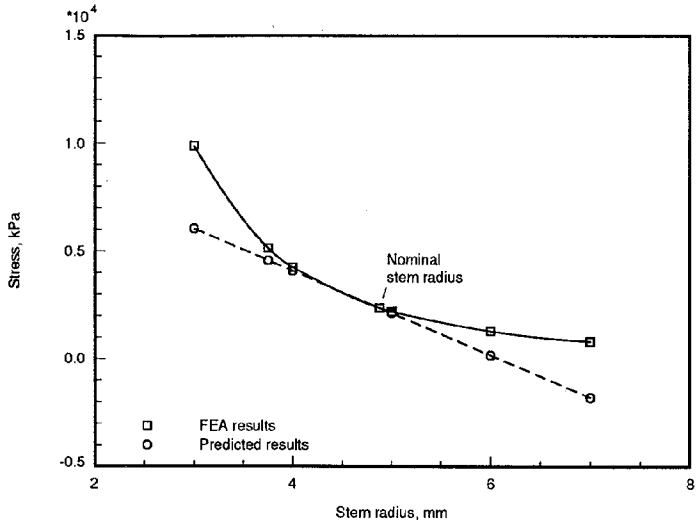

Figure 16: FEA results and sensitivity–based predictions (point loading)

predictions diminishes for values of stem radius that are far from the neighborhood of the nominal value.

It should be emphasized that the predictions of Table 1 were made based on the original FEA and the corresponding design sensitivity analysis (DSA). For this 2429 degrees of freedom structure, FEA and DSA took 3.0 and 2.9 minutes of CPU, respectively, on a DECstation 5000. Note also that the design changes are not limited to changes in a single dimensional parameter; i.e., the stem radius and the fillet radius can be changed simultaneously. Therefore, a linear model which allows prediction of stress with changes in the stem radius and/or fillet radius is built at a computational expense of 2.9 minutes, or roughly the expense of an additional FEA.

The predictions of Table 1 provide valuable insight on the behavior of the pin. In particular, it is apparent that σ_h has a significant dependence on the stem radius, but changes in the fillet radius are less important.

Case study: pin under gravitational loading

The loading is changed to a transverse gravitational loading to produce the stress distribution shown by Figure 17. Figure 18 shows the contour plot of $\frac{\partial \sigma_h}{\partial v_k}$ for the pin under gravitational loading. Comparison with Figures 13 and 14 suggests that in the fillet region, the sensitivities under gravitational loading are very similar to corresponding sensitivities under point loading.

However, the sensitivity distribution along the stem of the pin is quite different under gravitational loading. Figure 19 gives the sensitivities along the upper 2/3 of the stem for both loading conditions. Under point loading the sensitivity is zero for all NZS elements

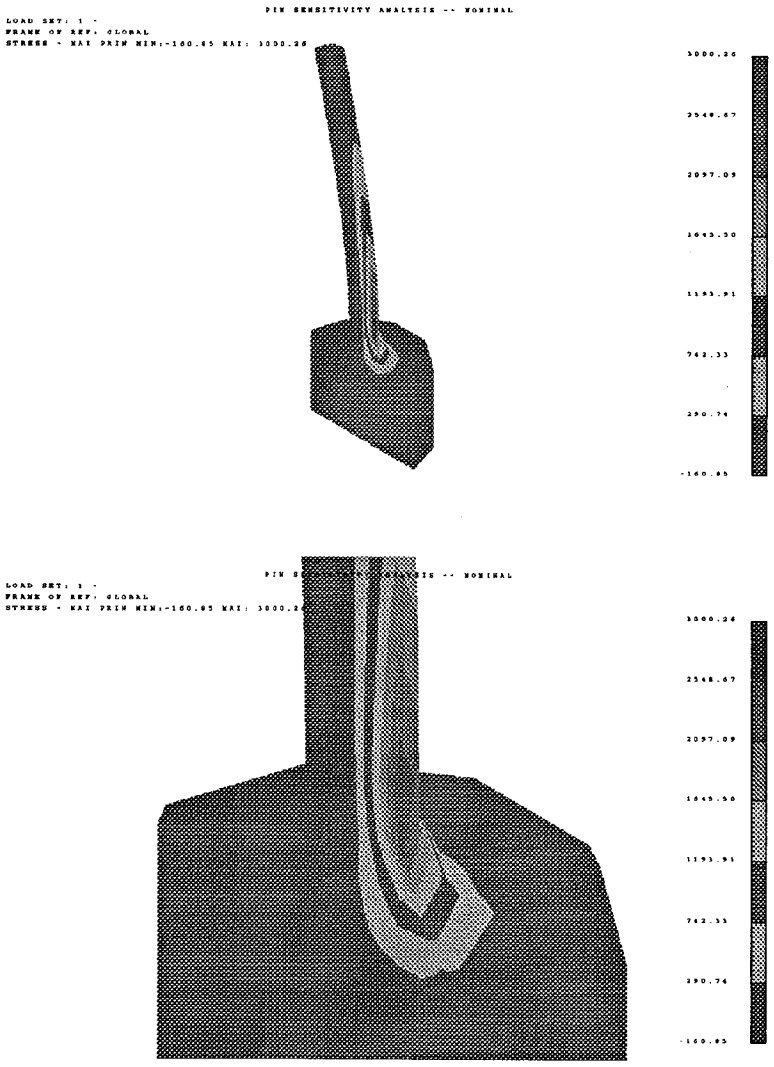

Figure 17: Maximum principal stress distribution (gravitational loading)

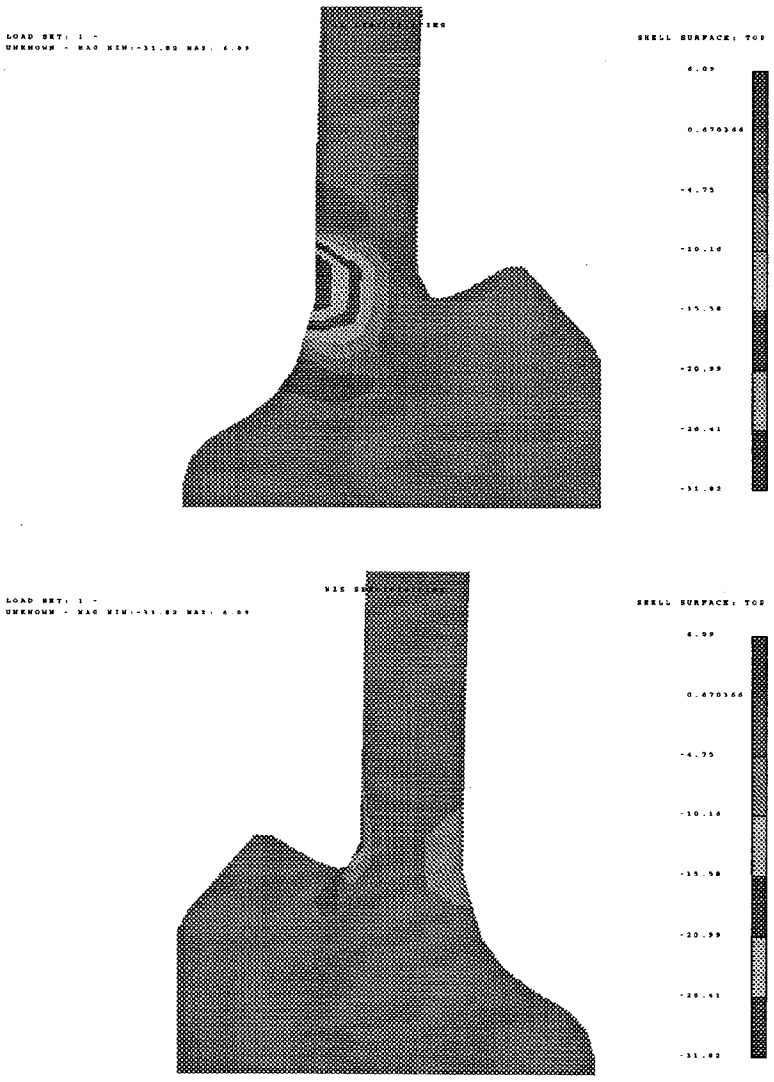

Figure 18: Sensitivity distribution (gravitational loading)

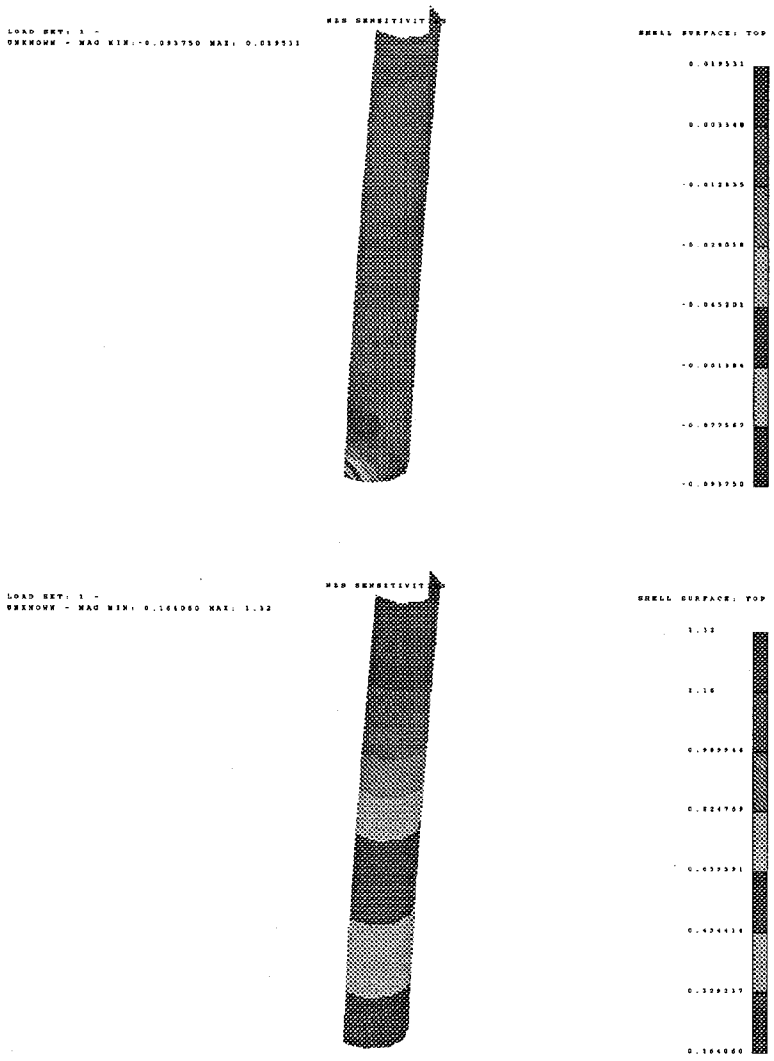

Figure 19: Sensitivity distribution along the upper 2/3 of the stem, tension side (point loading, top figure, and gravitational loading, bottom figure)

Table 2: Stress results for the pin geometry under gravitational loading

Design number	Stem radius (mm)	Fillet radius (mm)	FEA σ_h (kPa)	Predicted σ_h (kPa)	Deviation (kPa)
1 (nominal)	4.875	7.5	2371.2	—	—
2	3.75	7.5	3056.1	3504.4	448.3
3	3.75	5.0	3233.8	3437.2	203.4
4	6.0	5.0	2053.9	1170.9	883.0

which are far enough removed from the fillet region. For gravitational loading, the corresponding sensitivities are positive and assume their largest values at the free end of the pin. These sensitivities suggest that under gravitational loading, the predominant effect of additional material at the free end is to increase the loading which in turn has an unfavorable effect on the response.

The stem radius and fillet radius combinations of Table 1 are again used for the pin under gravitational loading. Table 2 presents the results. For ease of comparison, the magnitude of the gravitational loading is set such that σ_h for the nominal geometry is roughly equal to σ_h for the corresponding geometry under point loading.

As was the case with point loading, the predictions of Table 2 show that the stem radius has a larger influence on σ_h than the fillet radius. However, the level of this influence is less severe under gravitational loading. For example, from Design 1 to Design 2, where the stem radius is reduced from 4.875 mm to 3.75 mm, the stress due to the point load is predicted to increase from its nominal value of 2372.7 kPa to a value of 4574.3 kPa, while the corresponding predicted increase under gravitational loading is from 2371.2 kPa to 3504.4 kPa. Using Equation 3, this leads to:

$$\left.\frac{\partial \sigma_h}{\partial r_s}\right)_{point\ load} = -1957.0\ kPa/mm$$
$$\left.\frac{\partial \sigma_h}{\partial r_s}\right)_{grav.\ load} = -1007.3\ kPa/mm \tag{5}$$

where r_s represents the stem radius. This trend is expected since under a gravitational loading decreasing the stem radius has a dual effect of reducing the load as well as reducing the load carrying capacity, while under a point loading such a change only reduces the load carrying capacity.

Figure 20 presents the result of FEA runs corresponding to those given by Figure 16. Compared to the response under point loading, the stress versus stem radius relation exhibits a much more linear behavior under gravitational loading.

Under a gravitational load, the FEA and DSA for the nominal design required 3.2 and

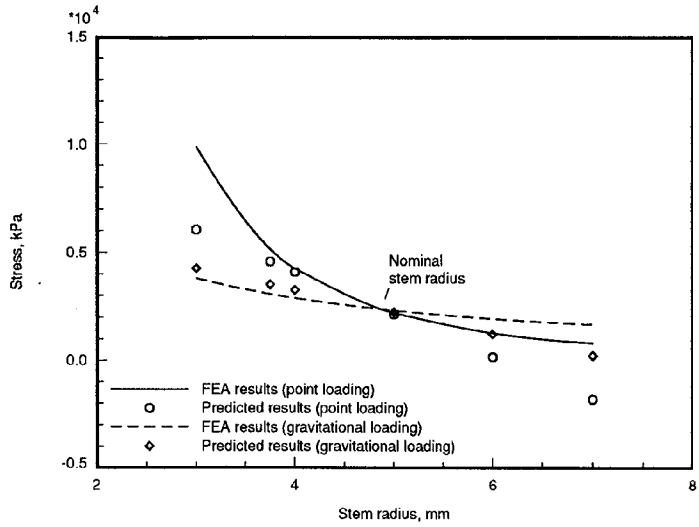

Figure 20: FEA results and sensitivity–based predictions (point loading and gravitational loading)

5.9 minutes of CPU, respectively, on a DECstation 5000 (compared with 3.0 minutes for FEA and 2.9 minutes for DSA under a point loading).

In summary, application of the parameter–based NZS method to the pin structure leads to the conclusion that the maximum tensile stress is much more heavily dependent on the stem radius than the fillet radius. It also shows that the dependence is stronger under a point load than a gravitational load.

Conclusions

This paper presented an extension of the shape optimization method introduced by Mikaili and Bernard [2] to design scenarios where the general shape characteristics of the structure must remain intact. Only relatively inexpensive size sensitivities are used.

The method is based on the introduction of a thin layer of elements, so–called NZS elements, on selected free surfaces of an existing finite element model of a structure. For structures modeled with solid elements, plate elements are used to coat the free faces of solid elements, while for structures modeled with plate elements, beam elements are used to line the free edges of plate elements. Since NZS elements are very thin, the incorporation of these elements does not significantly change the response of the structure. However, sensitivities of the response with respect to the thickness of these elements provide qualitative insight on the behavior of the structure as well as a quantitative basis for shape optimization.

Application of the method to a pin structure under two different static loading conditions showed that the method provides an effective and efficient basis for sensitivity–based shape optimization.

References

[1] Haftka, R. T., Grandhi, R. V. "Structural Shape Optimization–A Survey." Computer Methods in Applied Mechanics and Engineering 57 (1986): 97–98.

[2] Mikaili, A., Bernard, J. E. "Using Size Sensitivities to Guide Shape Redesign." MSC 1992 World Users' Conference Proceedings, Vol. 2.

[3] "I–DEAS Finite Element Modeling User's Guide, Version V, Structural Dynamics Research Corporation, Milford, OH, 1990."

[4] Vanderplaats, G. N., Numerical Optimization Techniques for Engineering Design: With Applications. McGraw-Hill, New York, 1984.

[5] Somayajula, G., Interactive Optimization of Mechanical Systems with Multiple Performance Requirements. Ph.D. Dissertation, Iowa State University, Ames, Iowa, 1989.